



[Article]

doi: 10.3866/PKU.WHXB201707031

www.whxb.pku.edu.cn

Effect of Pressure on Cesium Iodide Band Gap

CEDILLO Andrés^{1,*}, CORTONA Pietro²¹ Departamento de Química, Universidad Autónoma Metropolitana-Iztapalapa, San Rafael Atlixco 186, 09340 México, DF, México.² Laboratoire Structures, Propriétés et Modélisation des Solides, CNRS UMR 8580, Université Paris-Saclay, CentraleSupélec, Grande Voie des Vignes, F-92295 Châtenay-Malabry, France.

Abstract: The evolution of cesium iodide band gap as a function of pressure is studied in the range from 0 to 60 GPa. Within this range, two structural phase transitions occurred, and the band gap was affected by the compression pressure and structural rearrangement. The band gap estimation under pressure, as obtained by the density functional theory methods, successfully reproduced the experimental trend of the optical gap and electrical resistivity, namely, a general decreasing tendency, an early maximum, and a discontinuous peak around 40 GPa.

Key Words: Pressure-induced phase transition; Crystalline structure; Band gap; Resistivity

1 Introduction

Cesium iodide is an ionic solid with simple cubic crystal structure (B2 or CsCl-type) at room pressure and temperature; under these conditions, it is an insulator. This material attracted attention in the last decades when it was found that the isoelectronic solid xenon presents conducting features at high pressures^{1,2}.

Earlier experimental studies on cesium iodide showed that the B2 structure suffers a distortion under pressure and the band gap lowers^{3–14}. The structural phase transition from the B2 structure to a non-cubic one does not have a significant change in the volume and the order of the phase transition was under controversy. The high-pressure phase was initially assumed to be a tetragonal body-centered cell. The first theoretical studies showed that a tetragonal distortion on the B2 structure became stable at high pressures^{15–18,12,19–21}. A more precise X-ray diffraction study apparently finished with the controversy. Mao *et al.*²² proposed a pressure-induced continuous transformation from the B2 structure to a hexagonal close pack one (hcp) by an orthorhombic *Pmm2* cell. Later, the symmetry of the unit cell was corrected to *Pmma* by Winkler *et al.*²³. By the use of evolutionary codes, it was shown that the *Pmm2* structure is stable in a very small range of pressures (from 39 to 42 GPa) and it subsequently transforms into another orthorhombic cell with symmetry *Pnma*²⁴. The second phase transition is first order, however the change in the volume is minimal. Additionally, electric resistivity measurements at high pressures

were also performed and they showed that the resistivity decreases as pressure grows up, with a small discontinuity around 45 GPa^{25,26}. The variation of the CsI electronic properties with the pressure influences the use of this material as a photoelectrode^{27,28}.

Density functional theory (DFT) accurately predicts structural and energetic properties of molecular species and periodic solids. However, when the calculations are performed by the local density approximation (LDA) or using functionals belonging to the generalized-gradient approximation (GGA) class, the band gap of solids is usually underestimated. The accuracy of DFT in the prediction of the fundamental and the band gap has been analyzed in the literature^{29–31}. The electronic band gap is an important property of periodic solids since it determines the electric conductivity. Traditionally, materials are classified as conductors, semiconductors and insulators by the size of the band gap. Besides the accuracy of the DFT estimated band gap, this estimation provides an insight about the electric properties of a crystalline solid.

In this work we use DFT-based electronic structure methods to analyze the phase stability of cesium iodide and the evolution of the band gap in the range of pressures from 0 to 60 GPa, at zero temperature. Static cell estimations are reported and the zero point energy is not included in this study. The corresponding results are compared with the evolution of the resistivity along the compression.

Received: May 5, 2017; Revised: June 15, 2017; Accepted: June 23, 2017; Published online: July 3, 2017.

*Corresponding author. Email: cedillo@xanum.uam.mx; Tel.: +52-55-5804-6414.

A Lithuanian State Scholarship from the Education Exchanges Support Foundation was granted to A.C. Support from CONACYT grant 237045 and the hospitality of the SPMS Laboratory and Vilnius University were also acknowledged.

© Editorial office of Acta Physico-Chimica Sinica

2 Methodology

All the electronic structure computations have been done with the ABINIT code^{32,33} within the PAW formalism^{34,35} and using an energy cutoff of 30 hartree. The Brillouin zones were sampled by Monkhorst-Pack grids, which were shifted using the default shift option in the ABINIT code for all the phase stability analysis. For the B1 structure, the four shifts suggested on the ABINIT website were used. A $6 \times 6 \times 6$ grid was used for B1 and B2 structures, where the primitive cell contains one unit formula; for the *Pmma* cell we used the $4 \times 6 \times 4$ grid with two formula units; the *Pnma* cell contains four formula units and the grid $4 \times 4 \times 4$ was selected. The structure optimization was completed when the forces on all the atoms became smaller than 5×10^{-6} hartree-bohr⁻¹. For the evaluation of the band gap, once the convergence was achieved and the structures were optimized, one more calculation was performed. It was done using $12 \times 12 \times 12$, $8 \times 12 \times 8$, and $10 \times 10 \times 10$ grids, for the B2, *Pmma*, and *Pnma*, respectively. These grids were not shifted, in order to include the Γ point in the sampling.

The PBE exchange and correlation energy functional approximation was mainly used along this work³⁶. Some comparisons also involve the LDA and PBEsol³⁷ functionals. PAW atomic datasets for all the functionals were generated by the ATOMPAW code using the input files provided on the ABINIT website.

The *Pmma* and *Pnma* cells are shown in Figs.1 and 2, respectively, while the internal sites occupied by the ions are described in Table 1.

As we discussed above, several theoretical computations on CsI have been reported in the literature. However, the evolution

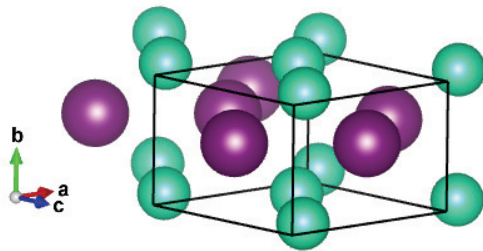


Fig.1 CsI in the orthorhombic *Pmma* structure.

The large purple spheres represent the iodide ions, while the small green ones correspond to the cesium ions. color online.

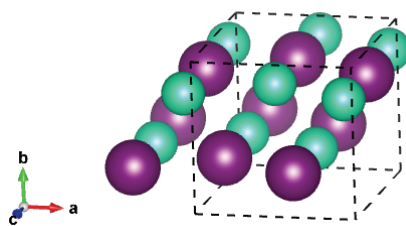


Fig.2 CsI in the orthorhombic *Pnma* structure.

The large purple spheres represent the iodide ions, while the small green ones correspond to the cesium ions. color online.

Table 1 Internal coordinates within the unit cell for the CsI orthorhombic structures.

Cell	<i>Pmma</i> (51)	<i>Pnma</i> (62)
Cs	Wickoff sites e	Wickoff sites 4c
I	Wickoff sites f	Wickoff sites 4c

of the experimental measurements mainly guided the direction of the electronic structure simulations in the early years. In this work, we compute the relative stability of all the relevant crystal phases and the pressure-effect on the band gap using DFT-based electronic structure methods under similar quality criteria. The selected *k*-point sampling meshes and plane-wave kinetic-energy cutoffs lead to convergence in the total energy and lattice parameters.

3 Results and discussion

The phase stability is analyzed by free energy, $G = E + PV - TS = H - TS$, of the different cell types, namely, NaCl-type (B1), CsCl-type (B2), and the orthorhombic cells *Pmma* (space group 51) and *Pnma* (space group 62). At zero temperature, the free energy becomes equal to the enthalpy (H). Then, for each pressure and for each cell type, the cell parameters and the internal coordinates are optimized. At zero pressure, the PBE functional approximation predicts that the B1 structure is the most stable; the B1 cell is lower in energy than the B2 cell by 2.3 mHa-formula⁻¹. Earlier reports also find a similar result³⁸. Different exchange and correlation energy functional approximations can overestimate the stability of some cells, see for example refs.39,40. The PBEsol approximation correctly predicts that the B2 cell is the most stable at low pressures and, at zero pressure, the B2 cell energy is lower than the corresponding one for the B1 structure by 0.3 mHa-formula⁻¹. This energy difference is within the thrust margin of predictability for an exchange and correlation energy functional approximation. As Mao *et al.* suggested²², the *Pmma* structure reduces to the B2 structure at low pressures. The two cell types become equivalent when $a = c$ and $a = \sqrt{2} b$. Using PBE one finds that the orthorhombic cell *Pmma* reduces to the cubic B2 below 38 GPa and this result is consistent with previous reports^{41,23,24}. Additionally, at low pressures, the orthorhombic *Pnma* cell becomes equal to the cubic B1 cell. PBE finds this symmetrization at 3 GPa.

As pressure increases, the enthalpy of the different phases changes and the stability is altered, see Fig.3. The B2 phase becomes more stable than the B1 at 0.6 GPa (PBE result). The PBE optimized lattice parameters for the different CsI phases are reported on Table 2. Note that PBEsol provides better estimation of the lattice parameter at zero pressure. The B2 phase is stable up to 38 GPa and it is equivalent to the *Pmma* cell. The *Pmma* cell becomes orthorhombic and more stable at moderate pressures. PBE predicts this transition at 38 GPa, where the lattice parameter ratios suddenly mismatched the

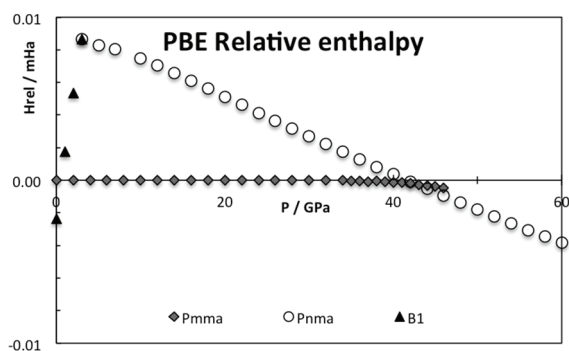


Fig.3 Relative enthalpy for the different CsI phases, PBE results in hartree·formula⁻¹.

Table 2 PBE lattice parameters for the different CsI structures.

Cell	Pressure/GPa	a/Å	b/Å	c/Å
B1	0	7.858		
B2	0	4.670		
Pmma	38	5.304	3.629	5.333
Pnma	44	5.678	5.330	6.422

The experimental lattice constant of CsI in the B2 structure, at room conditions, is 4.56 Å⁴. The LDA and PBEsol predicted lattice parameters at zero pressure are 4.409 and 4.514 Å, respectively. 1 Å = 0.1 nm.

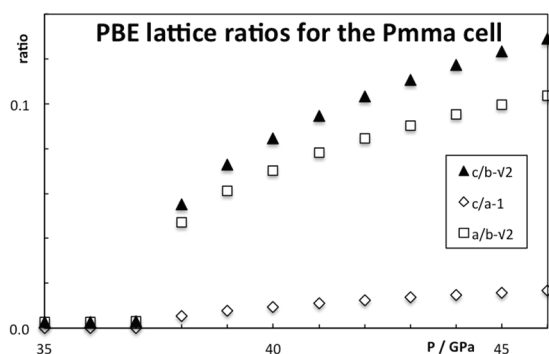


Fig.4 Deviation from the cubic symmetry in the CsI Pmma structure.

The ideal cubic value is subtracted from the lattice parameter ratios.

All the values correspond to the PBE results.

cubic conditions, see Fig.4. The phase transition seems to be first order, but the relative change in the volume is marginal, around 0.2%. The stability of the Pmma cell remains for a very limited range of pressures. The Pnma cell becomes the stable phase at higher pressures. Xu *et al.* predict the stability of this phase up to 300 GPa²⁴. PBE estimates that the orthorhombic Pnma phase becomes stable at 42.8 GPa and the phase transition is first order with a very small relative change in the volume, 1.4%. Even when two phase transitions are found between 38 and 43 GPa, the volume of the involved phases are so similar that the P - V curve seems to be almost continuous, Fig.5. The apparent continuous behavior of the isotherm is the main issue in the earlier controversy on the structural phase transition around 40 GPa. Some details on the crystal structures at the transition pressures are given in Table 3.

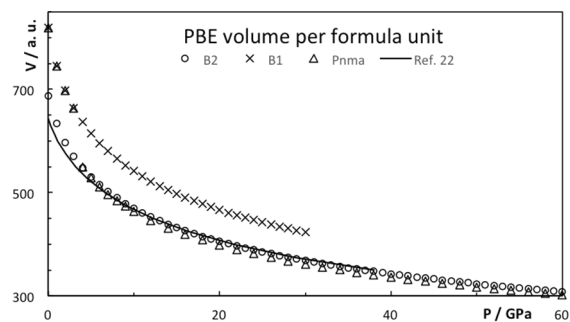


Fig.5 Volume per formula for the different CsI phases.

The fit to experimental P - V data from Mao *et al.*²² is shown by a continuous line.

In addition to the crystallographic and structural studies, electronic properties were also measured at high pressures. The pressure dependence of the optical gap^{3,4,10,12,14,42} and the electric resistivity^{25,26} were determined. Asaumi and Kondo³ originally observed that the threshold energy in CsI lowers as the pressure increases. Many efforts focused on the insulator-conductor transition and the band gap was estimated in different pressure ranges. Most of the studies report a decrease in the band gap with the pressure. Fig.6 shows the evolution of the electronic band gap, computed from the PBE functional approximation, with the pressure. At low pressures, the PBE method underestimates the band gap as it has been documented in the literature; however, the trend is correctly reproduced. In particular, a maximum value of the band gap is found around 2 GPa, $V/V_0 = 0.87$. The position of the maximum is in very good agreement with the results from Asaumi⁴. Other exchange-correlation energy functionals do not display necessarily the same behavior: PBEsol predicts a maximum at a similar pressure, while a monotonic decrease is obtained with LDA¹⁵. The discontinuity in the plot, around 43 GPa, is a consequence of the Pmma-Pnma phase transition. The Pnma structure presents a larger band gap, about 40 percent. The subsequent increase in the pressure leads a decrease in the band gap. This discontinuity can be mapped into the electric resistivity. Babushkin²⁵ found a sharp increase in the CsI resistivity around 45 GPa. At higher pressures, the electric resistivity monotonically vanishes, at least up to 220 GPa²⁶. These observations are consistent with our results for the estimated band gap. Our results also match previous theoretical reports^{15,17,23,24}. In fact, Xu *et al.*²⁴ predict that the gap vanishes

Table 3 PBE internal coordinates for the different CsI orthorhombic structures.

Cell	Pressure/GPa	Atom	x	z
Pmma	38	Cs		0.2212
		I		0.7234
Pnma	44	Cs	0.5912	0.3759
		I	0.5917	0.8759

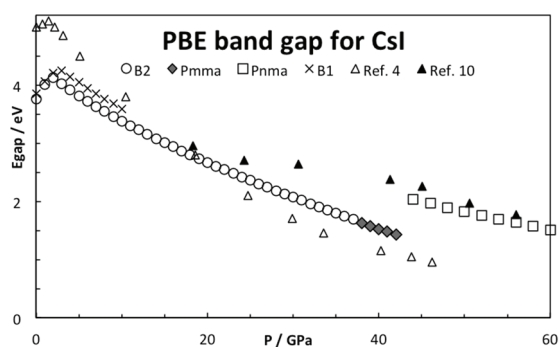


Fig.6 Effect of the pressure in the CsI band gap.

The experimental reported values are shown by triangles. Asaumi¹ reported threshold energies, which underestimate the band gap, while the values from Knittle and Jeanloz¹⁰ represent optical gaps. The experimental band gap of CsI, at zero pressure, is 6.135 eV⁴².

at 103 GPa from PBE computations, in excellent agreement with the experimental estimation of the band gap closure, around 100 GPa¹⁴.

4 Conclusions

DFT-based electronic structure methods provide a correct description of the structure, stability and pressure-induced phase transitions in CsI. The precision of these methods, especially at high pressures, is still under study for molecular and solid state systems. The PBE exchange and correlation energy functional approximation provides a good description of the relative stability of the different cell structures of CsI; however, it overestimates the stability of the B1 phase at zero pressure. The modified functional approximation for solids, PBEsol, corrects the phase stability problem, but it is not as accurate as PBE at high pressures. The authors previously observed this behavior in another crystalline system⁴⁰. A more extensive study of the performance of the different kinds of exchange and correlation energy approximations over a wide range of pressures could provide a more general conclusion.

The band gap prediction from DFT has also been under discussion for a long time. On a qualitative basis and assuming that the only relevant conduction mechanism comes from the band structure, it is interesting to notice that the band gap predictions from the PBE approximation favorably compare with the experimental measurements of the optical threshold energy and resistivity of CsI for the pressure range of this work. A quantitative estimation of the resistivity and the inclusion of thermal effects are beyond the scope of this study.

Acknowledgement: This work is dedicated to the memory of Robert G. Parr, a great scientist, humanist, and friend.

References

- (1) Nelson, D. A., Jr.; Ruoff, A. L. *Phys. Rev. Lett.* **1979**, *42*, 383. doi: 10.1103/PhysRevLett.42.383
- (2) Besson, J. M.; Itie, J. P.; Weill, G.; Makarenko, I. *J. Phys. Lett.* **1982**, *43*, 401. doi: 10.1051/jphyslet:019820043011040100
- (3) Asaumi, K.; Kondo, Y. *Solid State Comm.* **1981**, *40*, 715. doi: 10.1016/0038-1098(81)90813-9
- (4) Asaumi, K. *Phys. Rev. B* **1984**, *29*, 1118. doi: 10.1103/PhysRevB.29.1118
- (5) Huang, T. L.; Ruoff, A. L. *Phys. Rev. B* **1984**, *29*, 1112. doi: 10.1103/PhysRevB.29.1112
- (6) Itie, J.; Polian, A.; Besson, J. *J. Phys. Coll.* **1984**, *45*, 47. doi: 10.1051/jphyscol:1984809
- (7) Knittle, E.; Jeanloz, R. *Science* **1984**, *223*, 53. doi: 10.1126/science.223.4631.53
- (8) Huang, T. L.; Brister, K. E.; Ruoff, A. L. *Phys. Rev. B* **1985**, *30*, 2968. doi: 10.1103/PhysRevB.30.2968
- (9) Brister, K. E.; Vohra, Y. K.; Ruoff, A. L. *Phys. Rev. B* **1985**, *31*, 4657. doi: 10.1103/PhysRevB.31.4657
- (10) Knittle, E.; Jeanloz, R. *J. Phys. Chem. Solids* **1985**, *46*, 1179. doi: 10.1016/0022-3697(85)90147-7
- (11) Knittle, E.; Rudy, A.; Jeanloz, R. *Phys. Rev. B* **1985**, *31*, 588. doi: 10.1103/PhysRevB.31.588
- (12) Reichlin, R.; Ross, M.; Martin, S.; Goettel, K. A. *Phys. Rev. Lett.* **1986**, *56*, 2858. doi: 10.1103/PhysRevLett.56.2858
- (13) Vohra, Y. K.; Brister, K. E.; Weir, S. T.; Duclos, S. J.; Ruoff, A. L. *Science* **1986**, *231*, 1136. doi: 10.1126/science.231.4742.1136
- (14) Williams, Q.; Jeanloz, R. *Phys. Rev. Lett.* **1986**, *56*, 163. doi: 10.1103/PhysRevLett.56.163
- (15) Aidun, J.; Bukowinski, M. S. T.; Ross, M. *Phys. Rev. B* **1984**, *29*, 2611. doi: 10.1103/PhysRevB.29.2611
- (16) Christensen, N. E.; Satpathy, S. *Phys. Rev. Lett.* **1985**, *55*, 600. doi: 10.1103/PhysRevLett.55.600
- (17) Satpathy, S.; Christensen, N. E.; Jepsen, O. *Phys. Rev. B* **1985**, *32*, 6793. doi: 10.1103/PhysRevB.32.6793
- (18) Vohra, Y. K.; Duclos, S. J.; Ruoff, A. L. *Phys. Rev. Lett.* **1985**, *54*, 570. doi: 10.1103/PhysRevLett.54.570
- (19) Satpathy, S. *Phys. Rev. B* **1986**, *33*, 8706. doi: 10.1103/PhysRevB.33.8706
- (20) Baroni, S.; Giannozzi, P. *Phys. Rev. B* **1987**, *35*, 765. doi: 10.1103/PhysRevB.35.765
- (21) Cedillo, A.; Vela, A.; Gázquez, J. L. Structural Phase Transitions in Cesium Halides. In *Density Functional Methods in Chemistry*; Labanowski, J. K., Andzelm, J. W. Eds.; Springer: New York, NY, USA, 1991; pp. 293–306. doi: 10.1007/978-1-4612-3136-3_19
- (22) Mao, H. K.; Wu, Y.; Hemley, R. J.; Chen, L. C.; Shu, J. F.;

- Finger, L. W.; Cox D. E. *Phys. Rev. Lett.* **1990**, *64*, 1749.
doi: 10.1103/PhysRevLett.64.1749
- (23) Winkler, B.; Milman, V. *J. Phys. Condens. Matter* **1997**, *9*, 9811. doi: 10.1088/0953-8984/9/45/009
- (24) Xu, Y.; Tse, J. S.; Oganov, A.R.; Cui, T.; Wang, H.; Ma, Y.; Zou, G. *Phys. Rev. B* **2009**, *79*, 144110.
doi: 10.1103/PhysRevB.79.144110
- (25) Babushkin, A. N. *High Pressure Res.* **1991**, *6*, 349.
doi: 10.1080/08957959208201042
- (26) Eremets, M. I.; Shimizu, K.; Kobayashi, T. C.; Amaya, K. *J. Phys. Condens. Matter* **1998**, *10*, 11519.
doi: 10.1088/0953-8984/10/49/037
- (27) Breskin, A. *Nucl. Instrum. Meth. Phys. Res. A* **1996**, *371*, 116.
doi: 10.1016/0168-9002(95)01145-5
- (28) Va'vra, J.; Breskin, A.; Buzulutskov, A.; Chechik, R.; Shefer, E. *Nucl. Instrum. Meth. Phys. Res. A* **1997**, *387*, 154.
doi: 10.1016/S0168-9002(96)00980-1
- (29) Sham, L. J.; Schlüter, M. *Phys. Rev. Lett.* **1983**, *51*, 1888.
doi: 10.1103/PhysRevLett.51.1888
- (30) Perdew, J. P. *Int. J. Quantum Chem. Symp.* **1986**, *19*, 497.
doi: 10.1002/qua.560280846
- (31) Perdew, J. P.; Yang, W.; Burke, K.; Yang, Z.; Gross, E. K. U.; Scheffler, M.; Scuseria, G. E.; Henderson, T. M.; Zhang, I. Y.; Ruzsinszky, A.; *et al. Proc. Natl. Acad. Sci.* **2017**, *114*, 2801.
doi: 10.1073/pnas.1621352114
- (32) Gonze, X.; Amadon, B.; Anglade, P. M.; Beuken, J. M.; Bottin, F.; Boulanger, P.; Bruneval, F.; Caliste, D.; Caracas, R.; Côté, M.; *et al. Comput. Phys. Comm.* **2009**, *180*, 2582.
doi: 10.1016/j.cpc.2009.07.007
- (33) Gonze, X.; Rignanesel, G. M.; Verstraete, M.; Beuken, J. M.; Pouillon, Y.; Caracas, R.; Jollet, F.; Torrent, M.; Zerah, G.; Mikami, M. *et al. Z. Kristallogr.* **2005**, *220*, 558.
doi: 10.1524/zkri.220.5.558.65066
- (34) Blöchl, P. E. *Phys. Rev. B* **1994**, *50*, 17953.
doi: 10.1103/PhysRevB.50.17953
- (35) Torrent, M.; Jollet, F.; Bottin, F.; Zerah, G.; Gonze, X. *Comput. Mater. Sci.* **2008**, *42*, 337.
doi: 10.1016/j.commatsci.2007.07.020
- (36) Perdew, J. P.; Burke, K.; Ernzerhof, M. *Phys. Rev. Lett.* **1996**, *77*, 3865. doi: 10.1103/PhysRevLett.77.3865
- (37) Perdew, J. P.; Ruzsinszky, A.; Csonka, G. I.; Vydrov, O. A.; Scuseria, G. E.; Constantin, L.A.; Zhou, X.; Burke, K. *Phys. Rev. Lett.* **2008**, *100*, 136406.
doi: 10.1103/PhysRevLett.100.136406
- (38) Cortona, P. *Phys. Rev. B* **1992**, *46*, 2008.
doi: 10.1103/PhysRevB.46.2008
- (39) Demichelis, R.; Civalleri, B.; D'Arco, P.; Dovesi, R. *Int. J. Quantum Chem.* **2010**, *110*, 2260. doi: 10.1002/qua.22574
- (40) Cedillo, A.; Torrent, M.; Cortona, P. *J. Phys. Condens. Matter* **2016**, *28*, 185401. doi: 10.1088/0953-8984/28/18/185401
- (41) Buongiorno, M.; Baroni, S.; Giannozzi, P. *Phys. Rev. Lett.* **1992**, *69*, 1069. doi: 10.1103/PhysRevLett.69.1069
- (42) Lipp, M. J.; Yoo, C. H.; Strachan, D.; Daniels, W. B. *Phys. Rev. B* **2006**, *73*, 085121. doi: 10.1103/PhysRevB.73.085121